Penetration of the centrifugal barrier in the fusion of ^{16}O with heavy targets

R. Vandenbosch, B. B. Back,* S. Gil,† A. Lazzarini, and A. Ray
Nuclear Physics Laboratory, University of Washington, Seattle, Washington 98195
(Received 4 April 1983)

Gamma ray multiplicities and rotational band transition intensities have been measured for the $^{154}Sm(^{16}O, 4n)$ reaction for bombarding energies between 62.5 and 73.5 MeV. It is shown that centrifugal barrier penetration leads to a fairly broad spin distribution of the compound nucleus even at near-barrier energies. The results are discussed in terms of optical model absorption probabilities and parabolic barrier penetration probabilities.

[NUCLEAR REACTIONS Fusion $^{154}Sm(^{16}O,4n\gamma)$, $E=62.5-73.5$ MeV; measured $\sigma(E)$, rotational state populations. Deduced barrier parameters and mean compound nuclear spin values.]

I. INTRODUCTION

Total fusion (compound nucleus formation) cross sections for heavy ion induced reactions at near-barrier energies depend critically on the penetrability of the centrifugal plus Coulomb plus nuclear potential barrier. Many analyses of near or sub-barrier fusion cross sections employ the parabolic barrier approximation to account for the barrier penetration. In such analyses the penetrability coefficient $\hbar\omega$ in the Hill-Wheeler[1] penetrability expression characterizes the falloff in penetrability at sub-barrier energies. A number of recent calculations[2] or analyses[3,4] have employed $\hbar\omega$ values which are considerably larger than those obtained from matching the curvature of a parabolic barrier to that of a more realistic barrier such as given by a proximity[5] or Yukawa-plus-exponential nuclear potential.[6]

The penetrability of the barrier not only affects the dependence of the cross section on bombarding energy, it also affects the penetration of the higher partial waves at a given bombarding energy and hence the spin distribution of the compound nucleus. In the notation of a parabolic barrier, a larger value of $\hbar\omega$ implies greater penetration of the higher l waves and results in a broader spin distribution of the compound nucleus. The compound nuclear spin distribution plays an important practical role when one wants to use heavy ion reactions to probe fission dynamics or to synthesize unknown nuclear species. Branching ratios for n, p, α, and fission decay can depend sensitively on the compound nuclear spin distribution, as can fission fragment angular distributions. The latter are often analyzed assuming a sharp-cutoff model for determining the spin distribution. This assumption gets progressively worse as the mass of the projectile increases.

For these reasons it seems important to learn how to more quantitatively characterize the penetrability of the Coulomb plus centrifugal plus nuclear potential barriers. We report here a determination of the first moment of the compound nuclear spin distribution as a function of bombarding energy utilizing gamma ray multiplicities. We have also determined the relative intensities of the transitions deexciting the ground state rotational band, which provides information on the ground state band entry spin distribution.

II. EXPERIMENTAL

Oxygen beams were provided by the University of Washington two-stage FN Van de Graaff. Beam currents on target were limited to about 200 nA and by the GeLi singles rate. An Ortec 90 cm^3 GeLi detector was placed at 90° with respect to the beam and at a distance of 4 cm from the target. Two 7.6 by 7.6 cm NaI detectors were placed at 55° and 125° with respect to the beam and at a distance of 67 cm. These angles, corresponding to zeros of the Legendre polynominal P_2, were chosen to minimize angular distribution effects. A 0.75 mm thick lead and a 0.75 mm thick copper absorber were placed in front of each NaI detector. A silicon surface-barrier particle detector was placed at 40° and served as a monitor detector from which absolute cross sections could be determined. The efficiencies of the gamma ray detectors were determined by placing calibrated sources in the target position. An enriched target (^{154}Sm, 98.7%) of 500 $\mu g/cm^2$ thickness was used. Bombarding energies are corrected to the energy at the midpoint of the target.

The gamma ray multiplicities were determined from the ratio of the intensity of a particular γ transition in the GeLi spectrum in coincidence with any gamma ray in either of the NaI detectors to the intensity of the same transition in the singles GeLi spectrum through the relation

$$M_\gamma = \frac{N_\gamma^{\mathrm{GeLi}}(\mathrm{coinc}) \times C}{N_\gamma^{\mathrm{GeLi}}(\mathrm{singles})\epsilon^{\mathrm{NaI}}} + 1 ,$$

where the deviation of C from unity accounts for neutrons rather than gammas being detected by the NaI detector. We take C to be 0.9 on the basis of the work of Sie *et al.*[7] The total efficiency of the NaI detector was essentially constant for gamma ray energies above a few tenths of an MeV. Note that the GeLi detector efficiency does not enter into the multiplicity determination when using the present technique. The intensities of the ground state band rotational transitions were obtained from the GeLi singles yield using appropriate GeLi efficiencies determined by source calibrations.

III. GAMMA RAY MULTIPLICITIES

A. Results

The multiplicities obtained using the ^{166}Yb(4→2) transition as a gate are shown as a function of bombarding energy in Fig. 1. The reported multiplicities include a correction for the mostly unobservable (highly converted) 2→0 transition.

B. Conversion of gamma multiplicities to average angular momenta

It has been recognized for a long time that for heavy nuclei, where evaporated particles do not carry away much angular momentum, the gamma ray multiplicity depends linearly on the input angular momentum. Various studies have differed somewhat in the details of their treatment of the dependence of the angular momentum on gamma ray multiplicity. Many workers subtract off three or four gamma rays from the measured multiplicities before applying the proportionality constant between multiplicity and angular momentum. This correction is attributed to "statistical" gamma rays which do not carry away angular momentum and whose number is assumed to be independent of the input angular momentum. More recently Sie *et al.*[7,8] have shown that when one specifies a particular xn channel for which the multiplicity is being determined, as is the case in the present study, the number of statistical gamma rays depends on the total multiplicity. We have adopted an intermediate dependence for our particular case having measured total gamma ray multiplicities for cascades passing through the 4→2 transition, for which there must be a minimum multiplicity of two. We have compiled measured multiplicities for the (x,4n) reaction channel for a number of reactions leading to nuclei in the mass region under consideration.[7–9] We have considered only data taken at sufficiently high energies that barrier penetration effects are small. The relation $\bar{l}=1.58(M_\gamma-2)$ is consistent with this compilation. As an estimate of the uncertainty in this deduction of the average angular momentum from the measured multiplicities, we have considered two extreme possibilities. One of these is that none of the gamma rays are independent of input angular momentum, leading to a dependence given by

$$\bar{l}=1.31M_\gamma\ .$$

Alternatively, one might assume that there is a larger number of statistical gamma rays as determined by a least-squares fit to compiled data with no restraint on the intercept, leading to a dependence given by

$$\bar{l}=1.82(M_\gamma-3.3)\ .$$

The observed multiplicities have been converted to average angular momenta as indicated above and are plotted as a function of bombarding energy in Fig. 2. The error limits include both the uncertainties in the measured multiplicities and the uncertainties in the conversion to angular momenta as indicated above.

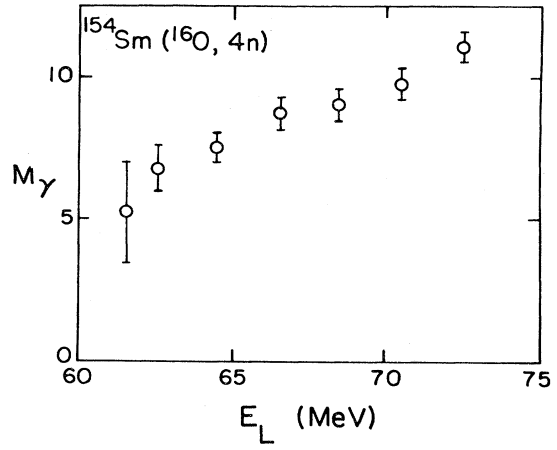

FIG. 1. Gamma-ray multiplicities for the ^{154}Sm(^{16}O,4n) reaction deexciting through the ^{166}Yb $4^+\rightarrow 2^+$ transition.

C. Comparison with theoretical expectations

1. Spin distribution from parabolic barrier approximation

A very simple and useful way to treat the probability for fusion is to approximate the combined nuclear and Coulomb potential barrier by an inverted parabola. The simplicity and utility of this approach result from the fact that the quantum-mechanical sub-barrier penetration and above-barrier transmission for a parabolic barrier are given exactly by a closed-form expression due to Hill and Wheeler,[1]

$$P=[1+e^{2\pi(E_B-E)/\hbar\omega}]-1\ .$$

The parameter $\hbar\omega$ is determined by the curvature of the barrier and by the inertial mass. E_B and $\hbar\omega$ can be estimated *a priori* by fitting parabolas to known potentials, and assuming that the inertial mass is given by the reduced mass. It should be noted, however, that the penetrability of potential barriers does not depend only on the curvature of the real part of the potential. Both the detailed shape of the real potential, and especially the strength and shape of an imaginary potential in the barrier region, significantly affect the sub-barrier penetrability, rendering a direct comparison of $\hbar\omega$ values somewhat unreliable. Commonly used nuclear potentials such as the proximity,[5] "Yukawa-plus-exponential,"[6] or Bass[11] model give $\hbar\omega$ values[3] of about four in the mass region under consideration. The centrifugal barrier is added by displacing the parabola upwards by the rotational energy for rigid spheres at a separation given by the position of the barrier maximum. Wong[12] has extended this approach to take into account target deformations. We have used his formalism with nuclear radii given by $r_i=1.2$ fm and an interaction barrier located at a separation given by $r_0=1.35$ fm. His equation (14) was integrated numerically to obtain the interaction barrier after an average over orientation angles.

We have used the fusion cross sections of Stokstad *et al.*[13] for ^{16}O+^{154}Sm to establish the barrier parameters. If one assumes ^{154}Sm to be spherical, a barrier height of 59

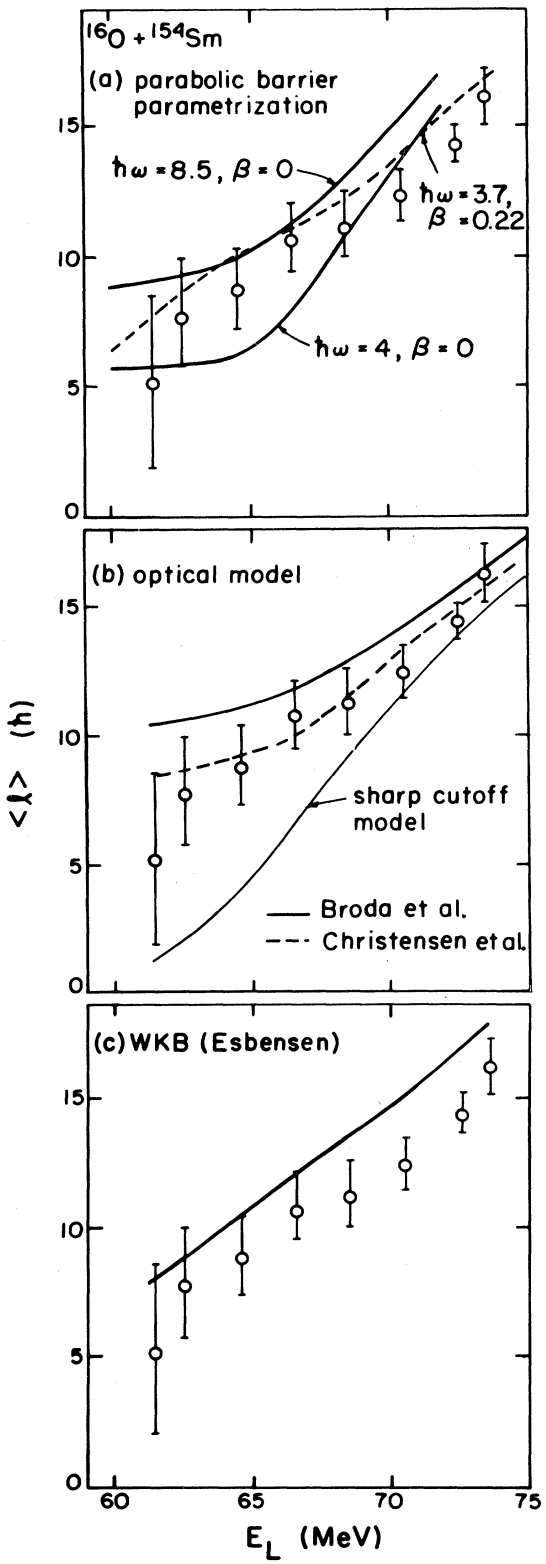

FIG. 2. Average momenta of the spin distributions leading to the $^{154}Sm(^{16}O,4n)$ reaction as deduced from gamma ray multiplicities are compared with (a) parabolic barrier penetration model predictions, (b) optical model and sharp cutoff model predictions, and (c) the WKB model of Esbensen including zero-point motions.

MeV and an $\hbar\omega$ of 8.5 reproduces the fusion excitation function fairly well, as shown in Fig. 3. This $\hbar\omega$ value, however, is approximately twice the *a priori* expectations. The cross section falls off much too fast as one decreases the bombarding energy if the expected value of $\hbar\omega \approx 4$ MeV is used. If one treats ^{154}Sm as being deformed, the fusion excitation function can be nicely reproduced with $\hbar\omega = 3.7$ and $\beta_2 = 0.22$, a value very close to that obtained by Stokstad and Gross[14] using a liquid-drop-model form factor for the nuclear potential and numerically solving the Schrödinger equation. This value of β_2 is somewhat smaller than that obtained by other methods (see Ref. 14). The bombarding energy dependence of $\langle l \rangle$ deduced from the $^{16}O + ^{154}Sm$ gamma ray multiplicities is compared with those calculated from various parabolic barrier prescriptions in Fig. 2(a). The calculations for a spherical target with $\hbar\omega$ of either 4 or 8.5 fails to account for the energy dependence of the data, whereas the calculation with $\beta_2 = 0.22$ and $\hbar\omega = 3.7$ accounts rather nicely for the data.

It is interesting to note that the same model which reproduces the fusion cross section of $^{16}O + ^{154}Sm$ also accounts quite well for very recently reported[15] fusion cross sections for $^{40}Ar + ^{154}Sm$. The insert to Fig. 3 shows a fit to these results with the same value of β_2, 0.22, and a similar value of $\hbar\omega$, 4.9.

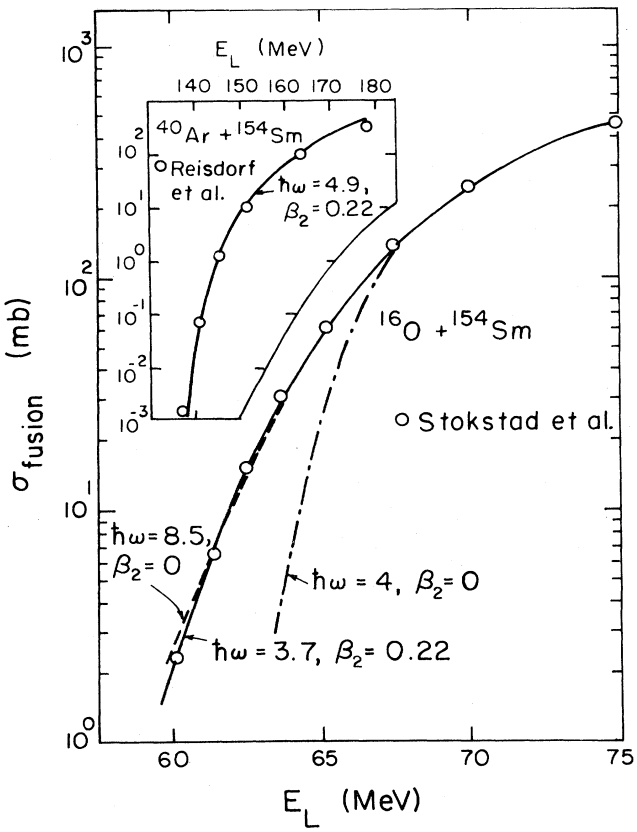

FIG. 3. Comparison of experimental fusion cross sections with various parabolic barrier models. The fits for ^{16}O and ^{40}Ar are obtained with barrier heights of 59 and 127 MeV, respectively.

2. *Spin distribution from optical model*

At these near-barrier energies most of the reaction cross section goes into compound nucleus formation. The only strong line seen in the GeLi gamma spectrum which does not originate from a compound nucleus product is the line corresponding to Coulomb excitation of the target. In the absence of any competing direct reactions, the optical model absorption cross section becomes equal to the fusion cross section, and the spin distribution is given by the absorption cross sections for the different partial waves. There are two difficulties in applying this approach. In the first place, most optical model potentials are obtained by fitting elastic angular distributions obtained at above-barrier energies, and do not automatically reproduce the total reaction cross section at lower energies. Secondly, direct reactions compete with compound processes for some of the absorption cross section, particularly at higher energies. We have therefore adopted the procedure of adjusting the partial-wave distribution attributed to fusion by shifting the grazing l so as to reproduce the absolute fusion cross sections. The diffuseness of the l distribution leading to fusion is assumed to be the same as that from the optical model absorption cross section. We have considered two optical potentials, a potential of Broda *et al.*[16] obtained by fitting elastic scattering of ^{16}O by ^{150}Nd and ^{12}C by ^{152}Sm, and a potential of Christensen *et al.*[17] obtained from the scattering of ^{16}O by ^{142}Nd. These potentials differ for a number of possible reasons. In the first study the experimental resolution was insufficient to resolve elastic scattering from inelastic scattering (mostly Coulomb excitation). Also ^{152}Sm and ^{150}Nd are deformed whereas ^{142}Nd is nearly spherical. The differences in the transmission coefficients for the two potentials, however, largely disappear when the shift to reproduce the measured fusion cross section is made. The mean angular momenta as a function of bombarding energy are compared in Fig. 2(b) with values obtained from the gamma ray multiplicities. When adjusted to reproduce the experimental fusion cross sections the $V=54$ potential of Broda *et al.*[16] and of Christensen *et al.*[17] give similar results and are in good agreement with experiment. The values predicted by the sharp cutoff model are considerably lower than experiment near the barrier. The differences in the predicted partial cross sections for the sharp-cutoff and optical[17] models are illustrated for two bombarding energies in Fig. 4. The optical model allows sufficient centrifugal barrier penetration for the higher partial waves to result in a much broader spin distribution and a higher average spin.

3. *Spin distribution from the WKB model including zero-point motions*

Esbensen[18] has developed a simple model for taking into account both zero-point motions (ZPM) and static deformations. The potential barrier penetration is calculated using a generalized Wentzel-Kramers-Brillouin (WKB) approximation. He previously fit the observed fusion cross sections for ^{16}O+^{154}Sm, using a permanent deformation of $\beta_2=0.225$ and adding the ZPM effects of the β and γ vibrations and octapole vibrations. The only parameter which was adjusted was ΔR, which was changed from its *a priori* value of 0.29 to 0.49 to fit the cross sections. The predicted $\langle l \rangle$ values with this adjusted value of ΔR are shown in comparison with the experimental values in Fig. 2(c). The results are rather similar to those calculated with the parabolic barrier representation with $\beta_2=0.22$ and $\hbar\omega=3.7$.

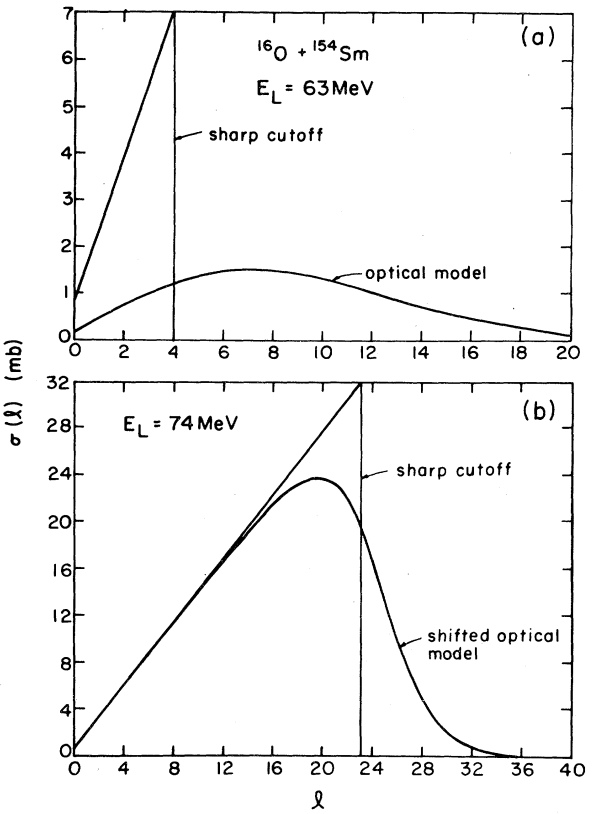

FIG. 4. Comparison of optical model and sharp-cutoff model compound nuclear spin distributions at 63 and 74 MeV.

IV. ROTATIONAL BAND POPULATION DISTRIBUTION

We were able to measure the intensities of the 4→2, 6→4, 8→6, and 12→10 lines in the Yb ground state band cascade. The 2→0 transition is highly converted and the 10→8 transition overlaps the 511 keV annihilation radiation line. The transition cross sections are displayed as a function of parent spin for several representative bombarding energies in Fig. 5. The absolute cross sections include a 1.2 angular distribution correction factor to convert the 90° yields to angle-integrated yields. These yields were parametrized by the expression

$$Y(J_i)=C/(1+\exp^{(J_0-J_i)/a}) .$$

A constant diffuseness of $a=3.5$ gave a reasonable description at all bombarding energies. The saturation

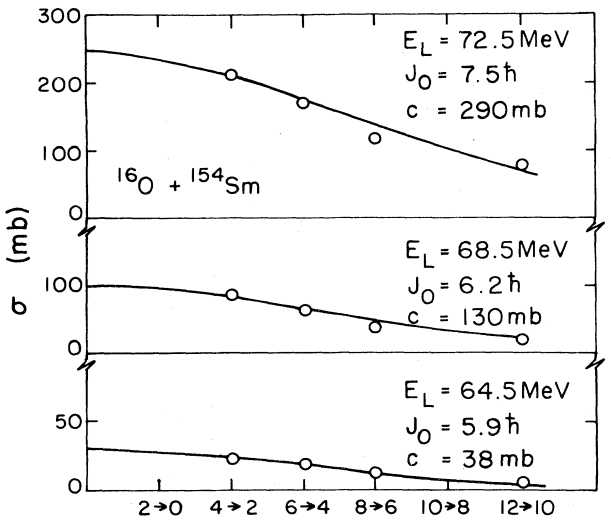

FIG. 5. Cross sections for deexcitation of specific rotational states at several bombarding energies. The relative errors are no larger than that corresponding to the size of the symbols plotted. The absolute uncertainties are less than 10%. The full curves are Fermi function fits as described in the text.

constant C and the mean entry spin J_0 values where the yield has fallen to half of the saturation value are given to the right of the curves. There was a consistent tendency for the $8\rightarrow6$ transition intensity to be slightly underpredicted and the $12\rightarrow10$ transition intensity to be slightly overpredicted. The cumulative yields extrapolated with the above formula to $J=0$ are compared with the results of Stokstad *et al.* in Fig. 6. The agreement is remarkably

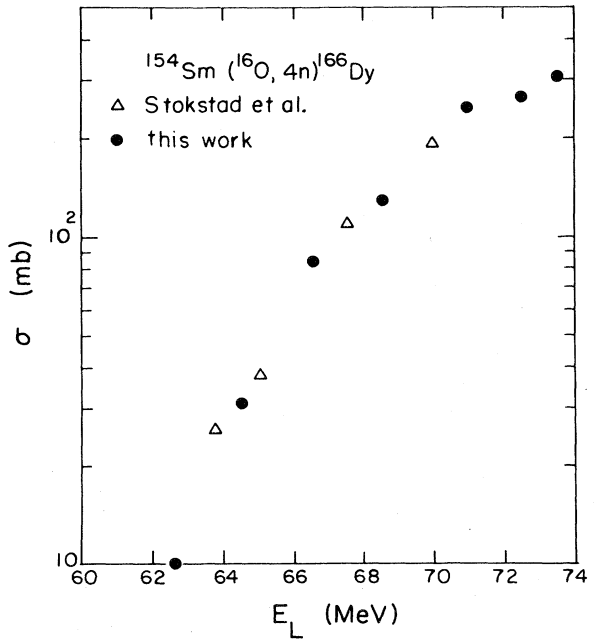

FIG. 6. Fusion cross sections deduced from the present measurements are compared with the results of Stokstad *et al.* (Ref. 13).

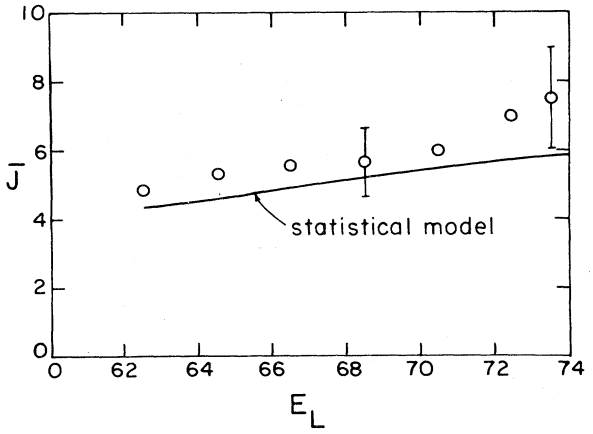

FIG. 7. Mean spin at entry of the ground state rotational band. The experimental points are based on fits to transition cross sections as in Fig. 5. The full curve is the result of a statistical model calculation.

good in as much as we used a relatively thick target and did not attempt a precise determination of the absolute yields. Our absolute cross sections have an uncertainty of 10—12 %, except at the 62.5 MeV where the uncertainty is 20%.

The mean values of the entry spin vary weakly with energy as shown in Fig. 7. These values can be qualitatively reproduced by statistical model calculations using the evaporation code PACE,[19,20] as shown in the figure. In contrast to the gamma ray multiplicities, the mean entry spin J_0 is not very sensitive to the input angular momentum distribution. The calculated values shown are based on an optical model spin distribution.

V. CONCLUSION

We have studied the gamma ray multiplicity and ground state rotational band feedings for the 4n channel in the $^{16}O+^{154}Sm$ reaction. This channel is dominant from near-barrier energies to considerably above-barrier energies. The gamma ray multiplicities, which are quite sensitive to the spin distribution of the compound nucleus, never decrease at low bombarding energies to the values expected if centrifugal barrier penetration were unimportant. The reduced mass of the entrance channel is sufficiently large for oxygen-induced reactions that a fairly large number of partial waves contribute nearly equally at even the lowest bombarding energies. The results of Fig. 4 indicate how erroneous the sharp-cutoff approximation can be. We have been able to achieve a fairly quantitative understanding of our results using either an optical model or penetration through a parabolic barrier approach. The simplicity of the latter together with the fact that one finds good agreement with *a priori* estimates of the penetrability coefficient makes this a useful approach for predicting the width of the spin distribution in unstudied systems. We find that if one averages over the orientation dependence of the static interaction barrier for the deformed target ^{154}Sm according to the procedure of Wong,[12] one can simultaneously account for both the ab-

solute fusion cross sections over several orders of magnitude and the mean value of the spin distribution over the same bombarding energy interval. We have found no need to invoke dynamic deformation or other more exotic effects. The feeding pattern of the ground state rotational band is less directly dependent on the initial compound nucleus spin distribution, but can be accounted for by statistical model calculations using a compound nucleus spin distribution consistent with the multiplicity observations.

ACKNOWLEDGMENTS

We thank S. Vandenbosch for assisting with the calculations. This work was supported in part by the U. S. Department of Energy under Contract DOE/ER/40048. One of us, B.B.B., is pleased to acknowledge the hospitality and support of the University of Washington Nuclear Physics Laboratory staff.

*Permanent address: Argonne National Laboratory, Argonne, IL 60439.

†On leave of absence form Comision Nacional de Energia Atomica, Buenos Aires, Argentina.

[1]D. A. Hill and J. A. Wheeler, Phys. Rev. 89, 1102 (1953).

[2]Q. Haider and F. Bary Malik, Phys. Rev. C 26, 162 (1982).

[3]U. Jahnke, H. H. Rossner, D. Hilscher, and E. Holub, Phys. Rev. Lett. 48, 17 (1982).

[4]K.-H. Schmidt, P. Armbruster, F. P. Hessberger, G. Münzenberg, W. Reisdorf, C.-C. Sahm, D. Vermeulen, H.-G. Clerc, J. Keller, and H. Schulte, Z. Phys. A 301, 21 (1981).

[5]J. Blocki, J. Randrup, W. J. Swiatecki, and C. F. Tsang, Ann. Phys. (N.Y.) 105, 427 (1977).

[6]H. J. Krappe, J. R. Nix, and A. J. Sierk, Phys. Rev. C 20, 992 (1979).

[7]S. H. Sie, R. M. Diamond, J. O. Newton, and J. R. Leigh, Nucl. Phys. A352, 279 (1981).

[8]S. H. Sie, J. O. Newton, J. R. Leigh, and R. M. Diamond, Phys. Rev. Lett. 46, 405 (1981).

[9]G. B. Hagemann, R. Broda, B. Herskind, M. Ishihara, S. Ogaza, and H. Ryde, Nucl. Phys. A245, 166 (1975).

[10]M. Ogaza, P. Kleinheinz, S. Lunardi, D. W. D. Schult, and M. Fenzl, Z. Phys. A 284, 271 (1978).

[11]R. Bass, Phys. Rev. Lett. 39, 265 (1977).

[12]C.-Y. Wong, Phys. Rev. Lett. 31, 766 (1973).

[13]R. G. Stokstad, Y. Eisen, S. Kaplanis, D. Pelte, U. Smilansky, and I. Tserruya, Phys. Rev. C 21, 2427 (1980).

[14]R. G. Stokstad and E. E. Gross, Phys. Rev. C 23, 281 (1981).

[15]W. Reisdorf, F. P. Hessberger, K. D. Hildenbrand, S. Hofmann, G. Münzenberg, K.-H. Schmidt, J. H. R. Schneider, K. Sümmerer, G. Wirth, J. V. Kratz, and K. Schlitt, Phys. Rev. Lett. 49, 1811 (1982).

[16]R. Broda, M. Ishihara, B. Herskind, H. Oeschler, S. Ogaza, and H. Ryde, Nucl. Phys. A248, 356 (1975).

[17]P. R. Christensen, I. Chernov, E. E. Gross, R. Stokstad, and F. Videbaek, Nucl. Phys. A207, 433 (1973).

[18]H. Esbensen, Nucl. Phys. A352, 147 (1981).

[19]The code PACE is a modification by A. Gavron of the code JULIAN, written by M. Hillman and Y. Eyal.

[20]A. Gavron, Phys. Rev. C 21, 230 (1980).